

# Spin-dependent hybridization and magnetic order of Ce/Fe(110) studied by spin-resolved resonant photoemission

Yu.S. Dedkov <sup>a,\*</sup>, M. Fonin <sup>b</sup>, Yu. Kucherenko <sup>c</sup>, S.L. Molodtsov <sup>a</sup>,  
U. Rüdiger <sup>b</sup>, C. Laubschat <sup>a</sup>

<sup>a</sup> *Institut für Festkörperphysik, Technische Universität Dresden, 01062 Dresden, Germany*

<sup>b</sup> *Fachbereich Physik, Universität Konstanz, 78457 Konstanz, Germany*

<sup>c</sup> *Institute for Metal Physics, National Academy of Sciences of Ukraine, 03142 Kiev, Ukraine*

---

## Abstract

Electronic and magnetic structures of the Ce/Fe(110) system were studied by means of spin- and angle-resolved resonant photoemission. Antiferromagnetic coupling of Fe 3d and Ce 4f spin magnetic moments was concluded from spin-resolved photoemission measurements supported by the electronic structure calculations. The relative intensity of the minority-spin component of hybridization feature at the Fermi level is larger than the majority-spin one, that can be assigned to spin-dependent hybridization between 4f and valence-band electrons induced by Fe substrate.

*Keywords:* Spin-resolved photoemission; LEED; Cerium; Hybridization

---

Compounds on the basis of rare-earth (RE) and transition-metal (TM) attract large interest due to their intriguing magnetic properties. Particularly compounds of the light REs Pr, Nd and Sm with late 3d elements find broad industrial applications [1]. For basic research, on the other hand, particularly magnetic instabilities are of current interest that lead, at low temperatures and in the neighborhood of so-called quantum-critical point, to phase transitions between magnetic order, superconductivity, and heavy-fermion behavior [2,3].

The electronic structure of RE–TM compounds is usually described within a standard model, where the 3d states are handled as itinerant by local spin-density approximation (LSDA), while the 4f states are treated as localized atomic-like states, split by crystal fields and indirectly exchange coupled via valence electrons. Interactions with valence electrons may also lead, however, to many-body

phenomena like mixed valence and Kondo-effect that cause a quenching of magnetic moments and counteract magnetic order. This competition is qualitatively well described by the Doniach diagram [4], where the ground-state depends on the relative values of the two characteristic energies: the Kondo condensation energy  $k_B T_K$  and the intersite RKKY exchange energy  $I$ . For small values of  $|J\rho(E_F)|$  ( $J < 0$  is the exchange coupling and  $\rho(E_F)$  is the density of states (DOS) at the Fermi level) the system is magnetic while, for high one, the Kondo effect dominates and the system is non-magnetic.

Starting from the picture of localized 4f electrons these phenomena may be described in the light of the Anderson model [5,6] by electron hopping between 4f and valence d orbitals. Particularly the single-impurity Anderson model (SIAM) [6,7], that treats the RE atoms as isolated impurities and ignores the translation symmetry of the lattice, has successfully been applied to many Ce and Yb systems [8,9]. SIAM predicts a strong dependence of electron hopping on the valence-band (VB) DOS close to the Fermi energy,  $E_F$ . Since the latter is usually large in transition-metal

---

\* Corresponding author. Tel.: +49 351 46335648; fax: +49 351 46333457.

*E-mail address:* dedkov@physik.phy.tu-dresden.de (Yu.S. Dedkov).

compounds and varies with spin-orientation in magnetically ordered systems, an interesting interplay between 4f exchange and hybridization may be expected.

While magnetization and transport measurements integrate over many electron states and excitation channels giving rather indirect information about the properties of the 4f states, most direct insight may be expected from photoemission (PE) that reflects the response of the electron system on a single 4f excitation. Particularly spin-resolved PE should be suited to study the interplay between magnetization and hybridization since both magnetic order and a possible spin-dependence of hybridization are reflected by the spin-resolved PE signal. Analysis of the 4f PE spectra in the light of SIAM allows for a determination of the ground-state properties the system. As has been shown recently [10–12], hybridization effects may vary with the emission angle reflecting a wave-vector dependence of hybridization. Quantitative description of this effect was possible in the light of a simple approach to periodic Anderson model (PAM) that in the limit  $U_{ff} \rightarrow \infty$  takes the form of SIAM with the main difference, that the VB-DOS used in SIAM is replaced by a  $\mathbf{k}$ -dependent energy distribution of valence states ( $U_{ff}$  denotes strong Coulomb interaction between f electrons). A spin-dependence of 4f hybridization was not studied up to now.

In the present work we report on the first spin- and angle-resolved resonant PE study of a structurally and magnetically ordered Ce/Fe(110) surface compound. A Ce–Fe system was chosen since these compounds are known to combine ferromagnetic order with strong hybridization of the 4f state [13]. A surface compound was selected in order to avoid problems related with (i) different hybridization strengths in the bulk and at the surface [14,15] and (ii) the non-conservation of the wave-vector component perpendicular to the surface. From the spin-asymmetry of the 4f emission an antiferromagnetic coupling of the 4f moments with respect to the Fe spins was concluded. The spectra reveal the characteristic double-peak structure of the Ce 4f emission, consisting of a “4f<sup>0</sup>” ionization peak at about 2 eV binding energy (BE) and a “4f<sup>1</sup>” hybridization feature at  $E_F$  [15]. The relative intensity of the latter with respect to the 4f<sup>0</sup> emission is larger for the minority than for the majority-spin direction pointing to a larger hybridization of those 4f states that are oriented antiparallel with respect to the Fe 3d moments. The PE data of the Ce/Fe(110) system are well reproduced within the periodic Anderson model using a LSDA slab calculation of La/Fe(110) and assuming spin and  $\mathbf{k}$  conservation upon hopping.

Ce/Fe(110) system was grown (at 130 K or room temperature) epitaxially on W(110) single crystal by deposition of high-purity Fe metal (thickness of about 50 Å) with subsequent annealing at 500 K followed by Ce films deposition (with the thickness of 0.5 monolayer assuming close-packed atomic arrangement) leading to a well-ordered surface structure (Fig. 1a and b). As it was shown by Kierren et al. [16] there is no noticeable interdiffusion

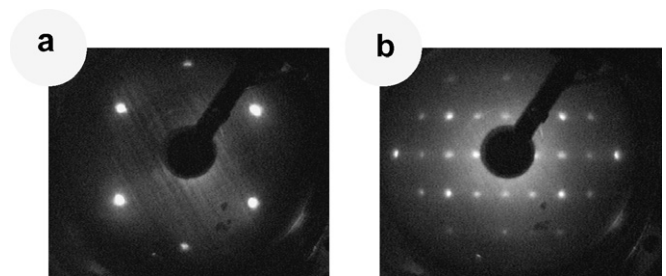


Fig. 1. LEED images of (a) pure Fe(110) surface and (b) ordered Ce/Fe(110) system.

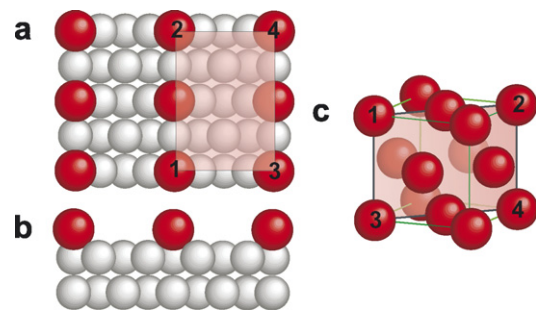


Fig. 2. Top (a) and side (b) views of the surface structure of the Ce/Fe(110) system. (c) Bulk unit cell of the fcc Ce.

at the Ce/Fe interface for the temperatures up to 300 K. Performed simulation by means of LEEDpat [17] package yields the surface structure shown in Fig. 2a and b. This structural model of the Ce/Fe(110) system gives a Ce–Ce neighbor distance increased by 11% as compared to bulk fcc  $\gamma$ -Ce [18] (magnetic ordering of Ce atoms could be prevailed). Spin- and angle-resolved resonant PE experiments at the Ce 4d  $\rightarrow$  4f absorption threshold were performed using a hemispherical PHOIBOS 150 electron-energy analyzer (SPECS) equipped with a 25 kV mini-Mott spin-detector (the effective Sherman function,  $S_{\text{eff}} = 0.1$ ) and synchrotron radiation from beamline U125/1-PGM of BESSY (Berlin). The total energy and angle resolutions were set to 100 meV and  $\pm 2^\circ$ , respectively. The light incidence angle was  $30^\circ$  with respect to the sample surface, and the photoelectrons were collected around the surface normal. Spin-resolved measurements were performed in normal emission geometry at 130 K in magnetic remanence after having applied a magnetic field pulse of about 500 Oe along the in-plane  $\langle 1\bar{1}0 \rangle$  magnetic easy axis (perpendicular to electric field vector of the light) of the Fe(110) film.

Electronic and magnetic structures of the Ce/Fe(110) system were probed by spin-resolved resonant PE at the Ce 4d–4f absorption edge. Unfortunately, in the photon energy range around Ce 4d–4f resonance the contribution of the Fe 3d PE to the total spectral intensity is considerable, unlike to the case of the most 4d and 5d TMs that have Cooper minimum of photoionization cross-section in this energy range [19]. However, taking into account a smooth energy dependence of the Fe 3d photoionization cross-section and that the spectral shape and the spin

polarization of Fe 3d photoelectrons are the same also at the resonance photon energies, the accurate separation of Ce- and Fe-contributions to PE spectra can be performed by careful normalization and subtraction of off-resonance spectra taken at  $h\nu = 112$  eV from on-resonance one at 121 eV.

Spin-resolved PE spectra of Ce/Fe(110) system measured at on- and off-resonance photon energies and the corresponding spin polarization as function of binding energy (BE), calculated as  $P = (I_{\uparrow} - I_{\downarrow}) / (I_{\uparrow} + I_{\downarrow})$ , are presented in Fig. 3 on the lower and upper panels, respectively. Here,  $I_{\uparrow}$  and  $I_{\downarrow}$  are majority-spin and minority-spin PE intensities marked by up- and down-triangles in Fig. 4 (lower panel). The difference in the spin-polarization curves measured at 4d–4f on- and off-resonance photon energies shows an effect of Ce atoms on the spin state of the outgoing photoelectrons.

In order to extract the Ce 4f contribution from observed PE spectra, the off-resonance PE spectrum (total intensity as well as majority- and minority-spin components) was subtracted from the on-resonance one. The resulted spin-resolved PE spectrum together with spin polarization of Ce 4f photoelectrons is shown in the lower panel of Fig. 4 (marked as ‘‘EXP.’’). The total Ce 4f PE spectrum shows a well-known two-peak structure, with a main maximum near 2 eV BE (‘‘normal ionization peak’’) and a hybridization peak near the Fermi energy [14,15]. The intensity ratio of these two-peaks indicates a weak  $\gamma$ -like hybridization of the 4f states with VB states, that is expected for the considered system due to larger Ce–Ce dis-

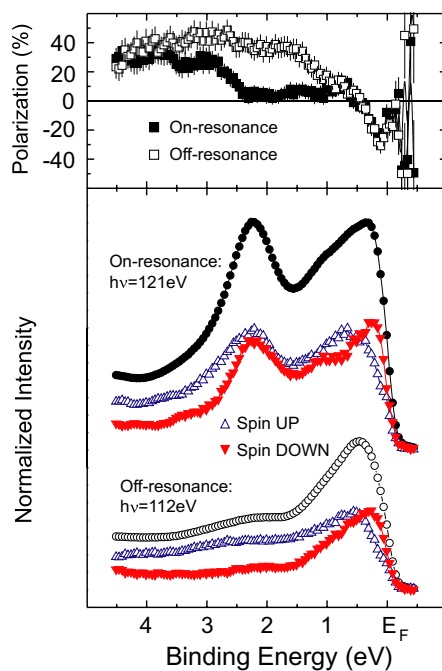


Fig. 3. Spin-resolved PE spectra (lower panel) and corresponding spin polarizations (upper panel) of Ce/Fe(110) system measured in on- and off-resonance at the 4d  $\rightarrow$  4f absorption threshold.

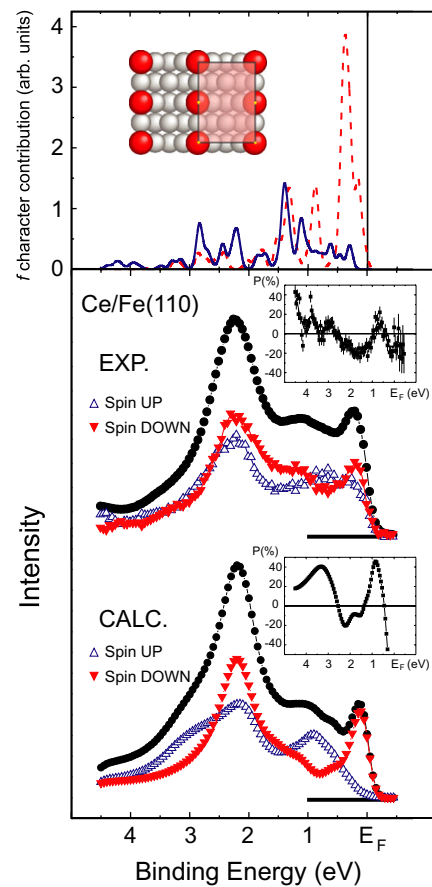


Fig. 4. (Upper panel) Calculated local 4f character of the VB states at the  $\Gamma$  point of the surface BZ for La/Fe(110). (Lower panel) Spin-resolved experimental and calculated Ce 4f emission for Ce/Fe(110) with corresponding spin polarizations shown as insets.

tances [11]. The spin-resolved components of this PE spectrum give a negative values of spin polarization at the energy positions of the two-peaks of Ce 4f emission. This could be a manifestation of preferred orientation of the Ce 4f spin magnetic moment opposite to the magnetization direction of Fe. It should be noted, that the intensity of hybridization peak is determined mainly by the minority-spin contribution, whereas for the majority-spin spectrum only a weak shoulder can be distinguished at this BE. Except of two main peaks, some other features are clearly resolved in the Ce 4f PE spectra: a shoulder near 1.2 eV BE in the minority-spin component and a maximum at 0.7 eV in the majority-spin one.

In order to explain the experimental spin-resolved PE spectra, we have performed the calculations of the electronic structure of the Ce/Fe(110) system. The atomic structure was chosen according to that shown in Fig. 2. The Fe substrate was simulated with a five-layer slab of Fe atoms with (110) orientation of the surface. The fully relativistic spin-polarized calculations were performed by means of the linear muffin-tin orbital (LMTO) method. A pure Fe surface as well as La/Fe(100) and Ce/Fe(100) systems were considered.

The La atom on the Fe(110) surface has a local spin moment of  $-0.24 \mu_B$ , determined mainly by 5d electrons ( $-0.20 \mu_B$ , the minus sign means the orientation antiparallel to Fe 3d spin moment). For Ce atom the local spin moment is equal to  $-1.12 \mu_B$ , with  $M_s(5d) = -0.28 \mu_B$  and  $M_s(4f) = -0.82 \mu_B$ . Thus, Ce 4f electron has preferred spin moment orientation opposite to the spin moment direction of the Fe atoms. However, on the other hand, the Ce 4f electron has a very high positive orbital moment of  $M_l(4f) = 2.80 \mu_B$ , so that the total moment of the Ce atom (taking into account all partially filled shells) is equal to  $M_{\text{tot}} = 1.70 \mu_B$ .

In order to describe the spin-resolved PE spectra, we used the simplified periodic Anderson model that was recently successfully applied to explain the angle-resolved PE spectra of CePd<sub>3</sub> [10] and Ce/W(110) system [11]. In this approach the double occupation of the 4f states is ignored and momentum conservation upon hybridization is assumed. For the spin-resolved PE spectra we assume additionally a spin conservation upon hybridization, i.e. no spin-flip processes for electron hopping between 4f state and VB (for details, please see [10,11,20]).

For the hybridization matrix element  $V_{\mathbf{k}}^{\sigma}(\varepsilon)$  of the two electron subsystems (VB and 4f states) we use the calculated respective f-projected local expansion coefficients  $c_f^{\sigma}(E, \mathbf{k})$  of the Bloch functions around the rare-earth sites:  $V_{\mathbf{k}}^{\sigma}(E) = \Delta \cdot c_f^{\sigma}(E, \mathbf{k})$ , where  $\Delta$  is an adjustable parameter ( $\mathbf{k}$  and  $\sigma$  are momentum and spin of electron, respectively;  $E$  denotes the BE of electron with respect to the Fermi energy). Expansion coefficients  $c_f^{\sigma}(E, \mathbf{k})$  that characterize the f character of VB states were taken from the results of the band structure calculations of the La/Fe(110) system, in order to exclude the contribution of localized Ce 4f orbitals. For normal emission of the photoelectrons we have to consider the VB states in the  $\Gamma$  point of the surface Brillouin zone. The calculated values of  $|c_f^{\sigma}(E, \Gamma)|^2$  are given in Fig. 4 (upper panel). The theoretical data are broadened by Gaussian ( $\Gamma_G = 50$  meV) for majority- (solid line) and minority-spin (dashed line) states. It can be seen, that the energy distributions of the VB f states are quite different for majority-spin and minority-spin electrons. These VB states of f symmetry in the La atomic sphere are created by combination of tails of wave functions of the neighboring atoms (mainly Fe 3d) and reflect (to some extent) their energy and spin distribution. This calculated VB f character causes strong differences in the hybridization matrix elements for majority-spin and minority-spin states resulting in different shapes of the 4f PE spectra for two spin directions.

The spectral functions for the Ce 4f emission were calculated using following parameters: the positions of non-hybridized f band are  $\varepsilon_f^{\uparrow} = -1.9$  eV,  $\varepsilon_f^{\downarrow} = -1.7$  eV and  $\Delta = 0.85$  eV. These numbers deviate from those obtained in Ref. [11] for Ce/W(110) system only by higher (about 0.5 eV) BE of the non-hybridized 4f level resulting from the lower coordination of the Ce atoms. An energy-dependent life-time broadening parameter of the form

$\Gamma_L = 0.03$  eV +  $0.085E$  was used. The calculated spectral functions were additionally broadened with a Gaussian ( $\Gamma_G = 100$  meV) to simulate finite instrumental resolution and an integral background was added to take into account inelastic scattering events.

The calculated spin-resolved Ce 4f PE spectra are presented in lower panel of Fig. 4 (marked as ‘‘CALC.’’). It agrees well with experimental spectra (Fig. 4, ‘‘EXP.’’) and reflects all features observed there. The minority-spin spectrum has much higher intensity of the hybridization peak near the Fermi energy due to high density of the minority-spin VB states at low BE. A shoulder near 1 eV BE is due to the hybridization effects with the peaks in the VB at 0.9 and 1.3 eV. In the calculated majority-spin spectrum no hybridization peak is observed, because of negligibly small density of VB states for this spin direction at the Fermi level. On the other hand, the ‘‘normal ionization peak’’ is split in three features (maxima at 0.9, 2.1, and shoulder at 3 eV) as a result of hybridization coupling with the VB states (the peak at 1.4 eV and the VB states between 2 and 3 eV).

The calculated spin polarization describes qualitatively the energy dependence of the measured one. Especially, there is a very good agreement for the points where the spin polarization changes the sign.

*In summary*, spin- and angle-resolved Ce 4f PE spectra of Ce/Fe(110) reveal a preferred antiparallel orientation of the Ce 4f spins with respect to the magnetization direction of the Fe substrate in agreement with results of a LSDA band-structure calculation. The spin-dependent shape of the Ce 4f spectra could successfully be simulated in the framework of a simple approach to PAM using the calculated LSDA band structure and assuming both spin and  $\mathbf{k}$  conservation upon hybridization. From our results, 4f-hybridization and, thus 4f-occupancy as well as net magnetic moment is generally expected to vary with spin-orientation, an effect that may be of crucial importance for the understanding of many-body phenomena in the neighborhood of quantum-critical points.

## Acknowledgements

This work was funded by the Deutsche Forschungsgemeinschaft, SFB 463, Projects TP B4 and TP B16 as well as SFB513. We acknowledge BESSY staff for technical support during experiment.

## References

- [1] See, for example: K.H.J. Buschow, Permanent Magnetic Materials and their Applications, Trans Tech Publications Inc., Zurich, 1998.
- [2] S.L. Sondhi et al., Rev. Mod. Phys. 69 (1997) 315.
- [3] S. Sachdev, Quantum Phase Transitions, Cambridge University Press, Cambridge, 1999.
- [4] S. Doniach, Physica B & C 91B (1977) 321.
- [5] P.W. Anderson, Phys. Rev. 124 (1961) 41.
- [6] O. Gunnarsson, K. Schönhammer, Phys. Rev. Lett. 50 (1983) 604.
- [7] R. Hayn et al., Phys. Rev. B 64 (2001) 115106.

- [8] Yu. Kucherenko et al., Phys. Rev. B 65 (2002) 165119;  
Yu. Kucherenko et al., Phys. Rev. B 70 (2004) 45105.
- [9] S.L. Molodtsov et al., Phys. Rev. B 68 (2003) 193101.
- [10] S. Danzenbächer et al., Phys. Rev. B 72 (2005) 033104.
- [11] D.V. Vyalikh et al., Phys. Rev. Lett. 96 (2006) 026404.
- [12] S. Danzenbächer et al., Phys. Rev. Lett. 96 (2006) 106402.
- [13] T. Konishi et al., Phys. Rev. B 62 (2000) 14304, and references therein.
- [14] C. Laubschat et al., Phys. Rev. Lett. 65 (1990) 1639.
- [15] E. Weschke et al., Phys. Rev. B 44 (1991) 8304.
- [16] B. Kierren et al., Phys. Rev. B 53 (1996) 5015.
- [17] The LEEDPAT program was written by K. Hermann, M.A. Van Hove and is available at <http://w3.rz-berlin.mpg.de/hermann/LEED-pat/>.
- [18] U. Kornstädt et al., Phys. Rev. B 21 (1980) 1898.
- [19] J.-J. Yeh, I. Lindau, At. Data Nucl. Data Tables 32 (1985) 1.
- [20] Yu.S. Dedkov et al., Phys. Rev. Lett., submitted for publication.